Hindawi
International Journal of Aerospace Engineering
Volume 2022, Article ID 1143901, 14 pages
https://doi.org/10.1155/2022/1143901

Research Article

Fatigue Reliability Analysis System for Key Components of Aero-Engine

Huizhi Qi,[1] **Yaqing Lu**,[1] **Shufang Song**,[1] **and Qiannan Xu**[2]

[1]*School of Aeronautics, Northwestern Polytechnical University, Xi'an 710072, China*
[2]*AECC Sichuan Gas Turbine Establishment, Mianyang 621700, China*

Correspondence should be addressed to Shufang Song; shufangsong@nwpu.edu.cn

Received 26 July 2022; Revised 25 September 2022; Accepted 26 September 2022; Published 14 October 2022

Academic Editor: Jinyang Xu

Copyright © 2022 Huizhi Qi et al. This is an open access article distributed under the Creative Commons Attribution License, which permits unrestricted use, distribution, and reproduction in any medium, provided the original work is properly cited.

Aero-engine is known as the heart of an aircraft. Fatigue is one of the main causes of aero-engine failure, therefore, it is essential to predict the fatigue life in the aero-engine design process. Due to the uncertainty of influencing factors, it is necessary to further analyze the fatigue reliability. First, the fatigue life should be predicted on the basic of finite element analysis. The steps include parametric modeling, stress-strain analysis, load spectrum acquisition, and selection of fatigue life prediction model. Then, the reliability estimation of fatigue life should be employed, including the statistical analysis of influencing factors, reliability analysis method, and reliability estimation of fatigue life. Taking turbine blade and test probe of aero-engine as the research objects, the fatigue reliability analysis system is developed based on the ABAQUS-MATLAB platform. Statistical analysis shows that fatigue life approximately obeys lognormal distribution, and the distribution parameters estimated by MCS and Kriging are coincide, while Kriging only needs dozens of training samples. Under different reliability indexes, the design fatigue life error between Kriging and MCS is less than 1%, which meets the accuracy requirements and can effectively guide the fault detection and maintenance of aero-engine.

1. Introduction

Aero-engine is the heart of an aircraft. If aero-engine failure occurs during the flight, it will be a direct threat to flight safety of the aircraft. And fatigue failure is one of the most typical failure modes of aero-engine [1], which will have a significant adverse effect on the safety, economic applicability, and equipment integrity of the aircraft. Therefore, it is very necessary to predict the fatigue life of aero-engine, especially its key components. Fatigue life prediction can provide reference for the service and maintenance cycle to ensure the stable operation of aero-engine [2].

Generally, according to stress levels or fatigue cycles, fatigue can be divided into high cycle fatigue (HCF) and low cycle fatigue (LCF). For HCF, the stress is low enough, the stress-strain relationship can be considered linear, and then S-N curve is commonly used to predict the fatigue life [3]. For LCF, the stress-strain relationship is hysteretic and nonlinear, and the local stress-strain method is the most widely used to estimate the fatigue life [4]. In fact, the fatigue problems of actual structure are often the superposition of several types of fatigue, such as high-low cycle complex fatigue (H-LCF). For example, H-LCF failure of the turbine blade accounts for 20% of aero-engine failures [5, 6].

Fatigue failure is a process of internal damage accumulation under cyclic stresses. Fatigue cumulative damage theory mainly includes linear and nonlinear cumulative damage theories. Miner's linear cumulative theory holds that the fatigue damage increases linearly with the number of cyclic stress. Because of its simple form and strong applicability, it is widely used in the fields of aerospace, transportation industry, and material science [7, 8, 9]. The nonlinear cumulative damage theory considers the coupling effect between different stresses [5, 10, 11], which is very theoretical, but it is too tedious to be applied to engineering problems.

Actually, the fatigue life is uncertainty due to geometric error and uncertainty of working environment [12, 13]. Therefore, it is necessary to analyze the fatigue life problem with probability statistics, that is, the reliability analysis of fatigue life [14, 15]. The probability distribution characteristics

of fatigue life should be obtained, such as distribution type 0. The numerical simulation method, represented by Monte Carlo simulation (MCS) 0, requires a large number of random samples to accurately predict the distribution of fatigue life, and it is time-consuming. How to improve the computation efficiency of fatigue reliability estimation has become an imperative issue. To address this issue, surrogate models, such as response surface method (RSM), neural network (NN), support vector machine (SVM), and Kriging model, have received widespread attention and rapid development [16–19]. Different from the aforementioned surrogate models, Kriging model can be established by using global and local information of training samples, including the information on the correlation between the variable of interest and covariates. Therefore, Kriging is a probabilistic prediction model with the unique advantage [20, 21]. The Kriging predictor is an unbiased and optimal predictor with smaller standard error to quantify the uncertainty than other surrogate models.

The fatigue life of aero-engine's key components, such as turbine blades and test probes, are predicted according to their different fatigue damage modes. Combined with the relevant knowledge of reliability, the fatigue reliability analysis framework is established by Kriging model. In addition, in order to realize the programming and automation of fatigue analysis, the corresponding simulation platform with strong readability and good operability is developed.

The rest of this paper is organized as follows: Section 2 presents the high-low complex fatigue life analysis model of aero-engine turbine blades and estimates the fatigue reliability under uncertain influence parameters. Section 3 establishes the high cycle fatigue analysis process and evaluates the corresponding reliability. Section 4 develops the fatigue life reliability analysis software platform based on ABAQUS-MATLAB. Section 5 summarizes the principles and advantages of the presented analysis framework and software platform.

2. Fatigue Reliability Analysis of Turbine Blade

Turbine blade of aero-engine is very prone to fatigue failure, since it works in very harsh working conditions: high-temperature, high-speed rotation, and high pressure complex environment. The content of blade fatigue reliability analysis includes finite element analysis to obtain the stress-strain response of dangerous position, H-LCF life prediction model, and fatigue reliability analysis.

2.1. Finite Element Analysis. First, finite element analysis is used to obtain the stress-strain response of the most dangerous position, which is the basic of the foundation for structural fatigue life prediction [22]. The steps of finite element analysis of blade are shown in Figure 1.

2.1.1. Parametric Modeling. There are 45 turbine blades in a turbine rotor, which are circumferential uniform distributed. The turbine blade is connected with the turbine disk through corresponding tenon. The geometric structure of blade is mainly composed of blade body, blade root platform, and tenon. In order to simulate the boundary conditions of turbine blades, the normal displacement of each tenon is limited, and the tenon foot is fixed. Considering that the blade has no rigid displacement, the normal displacement of the tenon side is also limited. The blade body uses C3D8R element type, the rest uses C3D10 element type, and the total number of grids is 12523. The boundary conditions of the blade are shown in Figure 2(a), the section of the blade body is shown in Figure 2(b), the finite element model is shown in Figure 2(c).

The turbine blade is made of K403 alloy, and the material parameters of K403 alloy [23] are listed as follows: the density is $8.10 \times 10^{-9} \rho(\mathrm{t/mm^3})$, the Elastic modulus is 165000 MPa, the Poisson's ratio is 0.33, and the thermal expansion coefficient is 1.38×10^{-5}.

2.1.2. Mechanics Analysis

(1) Load Analysis. The turbine blades have various loads, including centrifugal force, temperature load, aerodynamic load, and vibration excitation.

(1) Centrifugal load

The bottom of the turbine blade is fixed on the turbine disk under the action of the tenon, and centrifugal force is mainly the tensile stress produced by the quality of the blade itself in the process of high-speed rotation. In ABAQUS, the centrifugal force is directly applied by rotational speed at the central axis of turbine blade.

(2) Temperature load

Aero-engine turbine blades operate in a continuous high-temperature environment. The thermal stress is caused by the nonuniform temperature field and temperature change. The temperature field distribution of the turbine blade can be expressed according to the quadratic curve [24] as follows:

$$T(x) = T_a + (T_b - T_a)\left(\frac{x - R_a}{R_b - R_a}\right)^2, \quad (1)$$

where x represents the position of blade; R_a and R_b represent the distances from the highest point of blade body temperature and the lowest point of tenon temperature to the axis origin, respectively; T_a and T_b represent the maximum temperature of blade body and the minimum temperature of tenon, respectively.

(3) Aerodynamic load

The flow through the cascade channel causes aerodynamic loads. By analyzing the flow field characteristics, the aerodynamic force applied to the turbine blade is obtained from the pressure integration on the windward and leeward surfaces.

(4) Vibration load

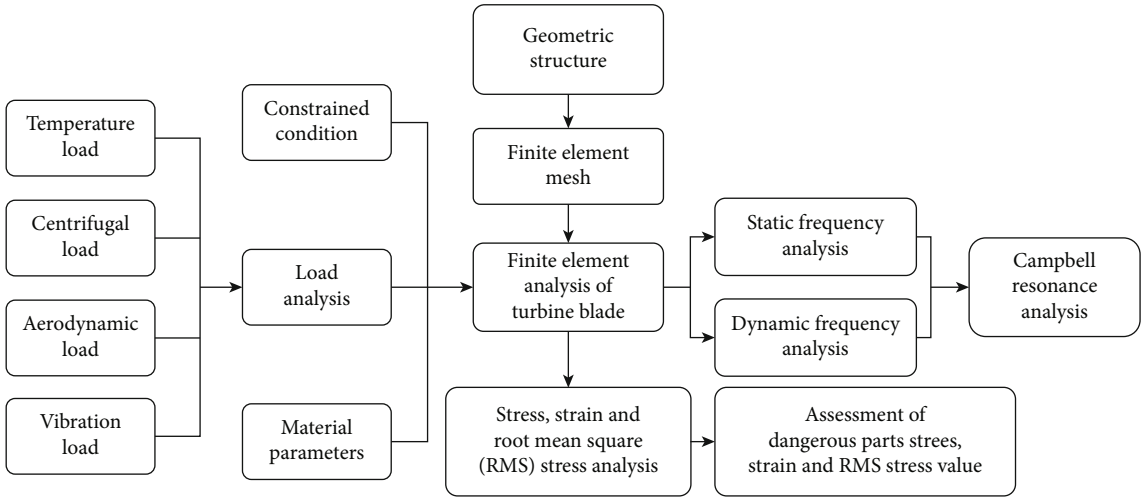

Figure 1: Flowchart of finite element analysis of blade.

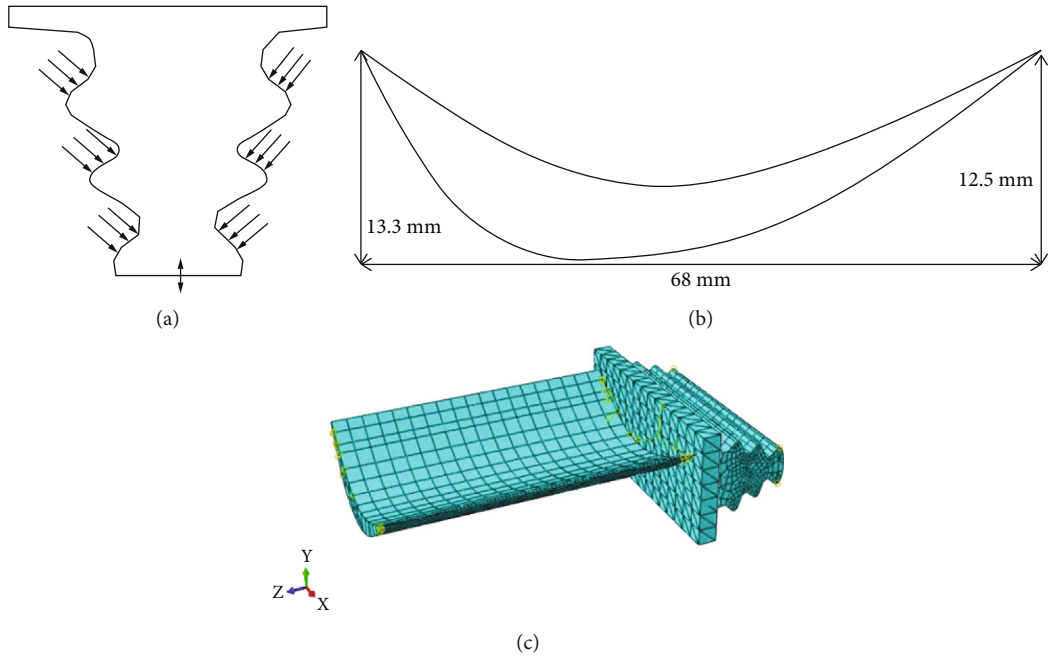

Figure 2: Turbine blade.

Table 1: 1000 h load spectrum of an aero-engine [25].

Working cycle	Cycle times (times)	Rotor speed (r/min)
Case 1	1280	0-17650-0
Case 2	1945	9210-17650-9210
Case 3	13300	16446-17650-16446

The airflow disturbance and turbine disk foundation vibration cause vibration loads. When the vibration excitation frequency is close to the natural frequency, the turbine blade is prone to resonance. Based on the flight test data, the fatigue cumulative damage to turbine blades under vibration load is calculated.

(2) Load Spectrum Analysis. Taking the rotational speed as the control quantity, the working states of aero-engine can be generally simplified as ground idling, cruising, and maximum-continuous. Then, there will be three key combination of working cycles: "start→maximum-continuous→-start," "Ground idling→ maximum-continuous→ground idling," and "cruising→maximum-continuous→cruising" (defined as case 1, case 2, and case 3, respectively). And it is assumed that the rotational speeds change uniformly between different working states. The load spectrum of aircraft flying 1000 h is shown in Table 1.

2.1.3. Static Finite Element Analysis. For the engine's three working states (ground idling, cruising, and maximum-

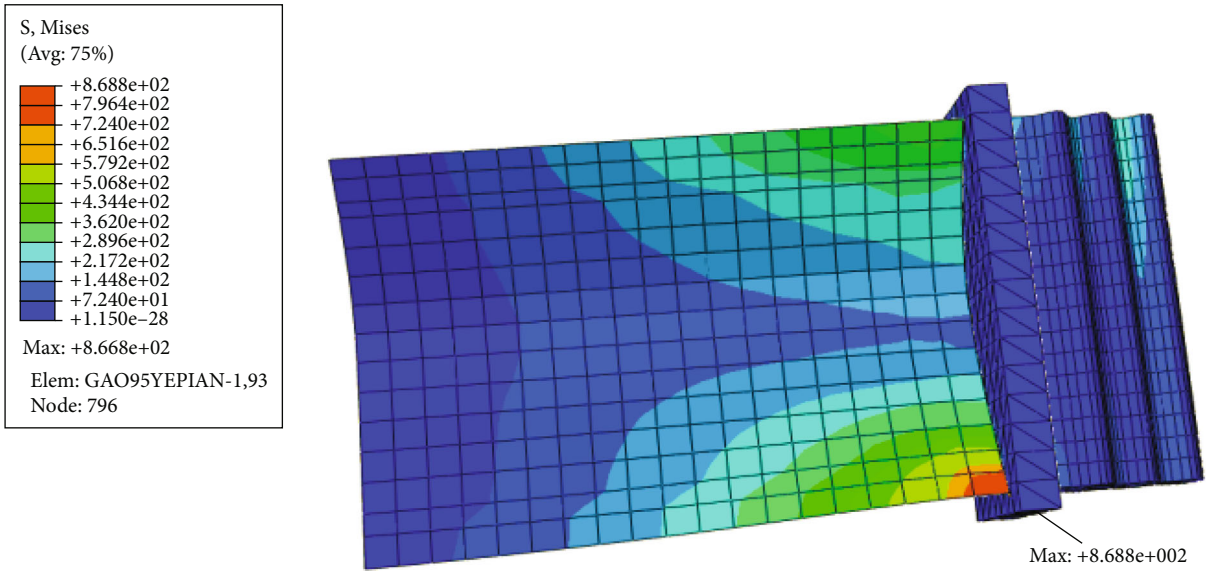

Figure 3: Stress cloud diagram of blade (maximum-continuous working state).

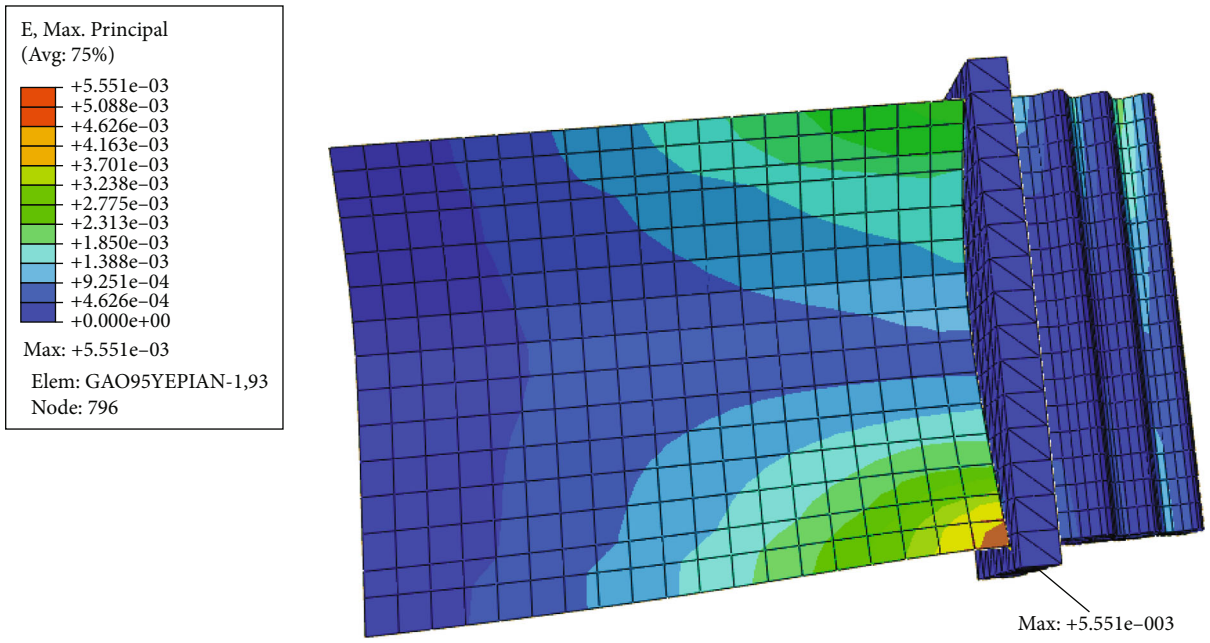

Figure 4: Strain cloud diagram of blade (maximum-continuous working state).

Table 2: Stress and strain results of three working states.

Working state	Stress (MPa)	Strain
Ground idling	692.67	0.002752
Cruising	796.93	0.003798
Maximum continuous	868.84	0.005551

continuous), the finite element stress and strain analysis of the turbine blade were carried out. The stress cloud diagram and strain cloud diagram of the blade structure are shown in Figures 3 and 4. The stress field is reasonably distributed, and the high stress area is concentrated at the root of the blade body. The stress and strain results are listed in Table 2.

2.1.4. Vibration Analysis. Structural resonance is one of the most dangerous causes of fatigue failure under vibration load. When the frequency of external excitation load is close to the natural frequency of structure, resonance will occur.

The static frequency is only related to the material properties and geometric structure of the turbine blade. The dynamic analysis is to calculate the natural vibration frequency of the turbine blade with working loads as prestress input. The results of static frequencies and natural frequencies of each working state are shown in Table 3.

Table 3: Calculation results of turbine blade frequencies.

	1st	2nd	3rd	4th	5th	6th
Static	816.19	1025.4	1911.0	1981.6	3081.5	3357.8
Ground idling	811.98	1024.3	1910.1	1964.3	3085.5	3359.3
Cruising	789.33	1002.2	1827.3	1895.4	3074.4	3339.5
Maximum-continuous	751.04	1006.4	1713.5	1869.6	3040.6	3304.7

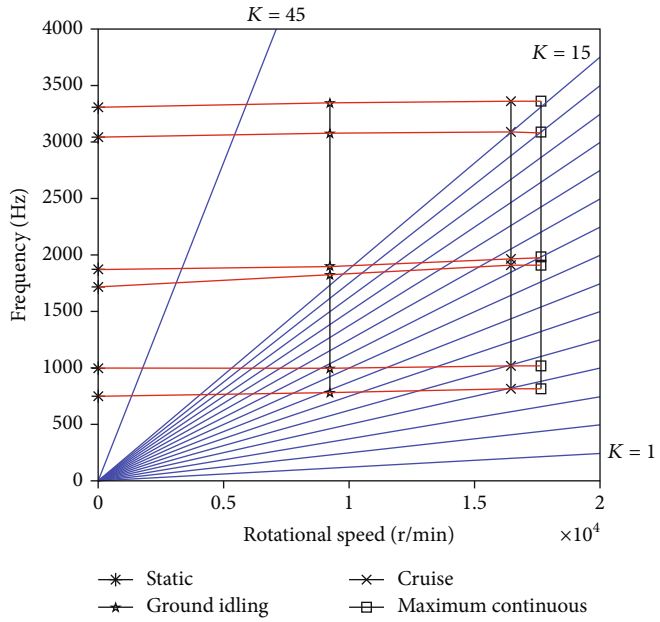

Figure 5: Campbell diagram.

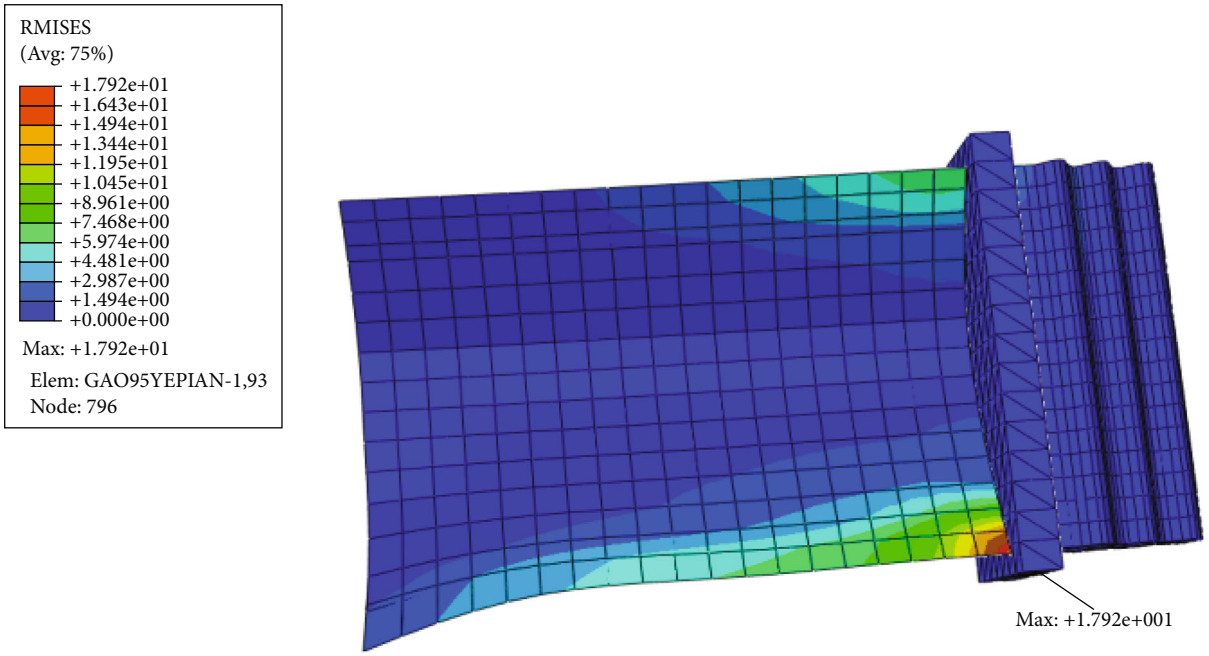

Figure 6: RMS stress cloud diagram.

Table 4: Calculation results of turbine blade life.

Fatigue life	Case 1	Case 2	Case 3
N_L	11160.0691	234517.9719	1647855.2250
N_H	6.1995×10^6	3.5470×10^7	2.1666×10^8

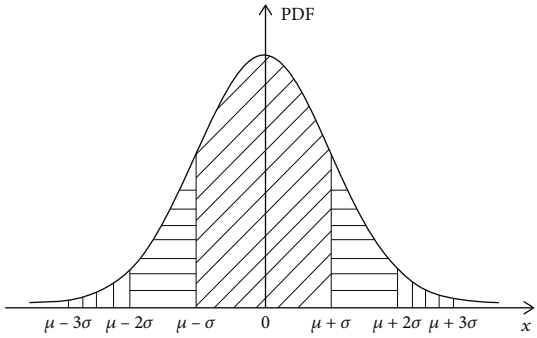

Figure 7: Interval division diagram.

The Campbell diagram is an overall view of regional vibration excitation that can occur in the blade's working states [26]. That is to say, judge whether the running frequency or its harmonics causes the resonance of the blade natural frequency. The engine rotational speed is along X axis, and the frequency is along Y axis. The fan lines are the excitation order lines from $K = 1$ to $K = 15$ and $K = 45$. As shown in Figure 5, turbine blades have resonance risks under excitation orders of 4, 5, 9, 14, and 15.

And then it is necessary to calculate the fatigue cumulative damage caused by low amplitude and high frequency vibration load. The frequency domain method based on power spectral density (PSD) is adopted. Setting the PSD of vibration load as input, the structural vibration response can be obtained through structural dynamic analysis. The RMS stress cloud diagram of turbine blade is shown in Figure 6.

2.2. High-Low Cycle Complex Fatigue Life Prediction. Turbine blade bears high and low cycle loads at the same time, and it is a complex fatigue problem. Turbine blade's LCF and HCF are analyzed firstly and then need to be comprehensively considered to predict its H-LCF life.

2.2.1. Low Cycle Fatigue Life Prediction Model. The local stress-strain method is usually used to predict the LCF life. The Manson-Coffin model modified by SWT (Smith-Watson-Topper) considers the effects of plastic strain and average stress on the fatigue life of turbine blades. The expression of SWT modified model is as follows:

$$\sigma_{\max}\varepsilon_a = \frac{\sigma_f'^2}{E}(2N)^{2b} + \sigma_f'\varepsilon_f'(2N)^{b+c}, \quad (2)$$

where $\sigma_{\max}$ is the maximum stress and ε_a is the strain amplitude. The fatigue performance parameters are calculated by the improved universal slope method [3] as follows:

$$\begin{cases} \sigma_f' = 0.623E\left(\dfrac{\sigma_b}{E}\right)^{0.832}, \\ \varepsilon_f' = 0.0196\left(\dfrac{\sigma_b}{E}\right)^{-0.53}. \end{cases} \quad (3)$$

For K403 alloy, the fatigue strength coefficient $\sigma_f' =$ 1401MPa, fatigue strength index $b = -0.09$, fatigue ductility coefficient $\varepsilon_f' = 0.329$, and fatigue ductility index $c = -0.56$. Newton iterative method can be used to solve Eq. (2). The fatigue limit life $N_{Li}(i = 1, 2, 3)$ under three working cycles can be obtained and listed in Table 4. Miner's linear cumulative damage theory is employed to calculate the total LCF damage $D_L = \sum_{i=1}^{3}(n_i/N_{Li})$, and the total LCF life is $N_L = 1/D_L \approx 7.63$, that is to say, the LCF life is 7630 h.

2.2.2. High Cycle Fatigue Life Prediction Model. Steinberg [27] proposed three-interval method based on the Gauss distribution and Miner's cumulative damage criterion to analyze the HCF life. Considering the random vibration excitation as Gauss distribution, then, the probability of three intervals is $P(|x - \mu| \le \sigma) = 68.3\%$, $P(\sigma < |x - \mu| \le 2\sigma) = 27.1\%$, $P(2\sigma < |x - \mu| \le 3\sigma) = 4.33\%$, and $P(|x - \mu| > 3\sigma) = 0.27\%$ (seen in Figure 7).

That is to say, the damage caused by vibration load in interval $|x - \mu| > 3\sigma$ can be ignored. Then, the calculation formula for HCF damage is as follows:

$$D_{H_i} = \frac{n_{1\sigma}}{N_{1\sigma}} + \frac{n_{2\sigma}}{N_{2\sigma}} + \frac{n_{3\sigma}}{N_{3\sigma}} = \left(\frac{0.683f}{N_{1\sigma}} + \frac{0.271f}{N_{2\sigma}} + \frac{0.0433f}{N_{3\sigma}}\right) \times T, \quad (4)$$

where D_{H_i} is the cumulative damage of HCF caused by vibration load; $N_{1\sigma}$, $N_{2\sigma}$, and $N_{3\sigma}$ are the cycle numbers corresponding to 1σ, 2σ, and 3σ stress level from S-N curve; f is the first order natural frequency of structural vibration; T is the total vibration time.

For the turbine blade, the maximum equivalent stress σ = 17.92 MPa. The S-N curve of the material can be obtained by querying the Handbook of Aeronautical Materials of China [23]. Query the corresponding allowable cycle times $N_{1\sigma}$, $N_{2\sigma}$, and $N_{3\sigma}$ under 1σ, 2σ, and 3σ stress, and substitute them into Eq.(4) to calculate D_{Hi}. Set the cumulative critical as 1, the HCF life will be $N_{Hi} = 1/D_{H_i}$, as shown in Table 4. And the total HCF damage $D_H = \sum_{i=1}^{3} D_{H_i} = \sum_{i=1}^{3}(n_i/N_{Hi})$, the HCF life is 3098950 h.

2.2.3. High-Low Cycle Complex Fatigue Life Prediction Model. Considering the coupling between HCF loads and LCF loads, the dual-parameter modified nonlinear damage accumulation model, proposed by Yue [5], is used to estimate the complex fatigue life.

$$N_{HL} = \frac{a_{HL}}{(1/N_L) + (1/N_H) + A_{HL}(1/N_L)^{1-B_{HL}}(1/N_H)^{B_{HL}}}, \quad (5)$$

Table 5: Statistical characteristics of random variables.

Random variable	Distribution type	Mean value	Coefficient of variation
1st rotation speed ω_1 (r/min)	Normal	17650	0.02
2nd rotation speed ω_2 (r/min)	Normal	16446	0.02
3rd rotation speed ω_3 (r/min)	Normal	9210	0.02
Young's modulus (MPa)	Normal	165000	0.01
Poisson's ratio	Normal	0.33	0.01
Thermal expansion coefficient	Normal	1.38×10^{-5}	0.01

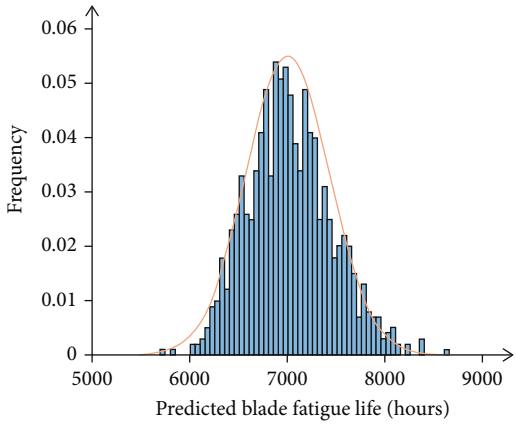

Figure 8: Distribution of fatigue life samples (Monte Carlo method).

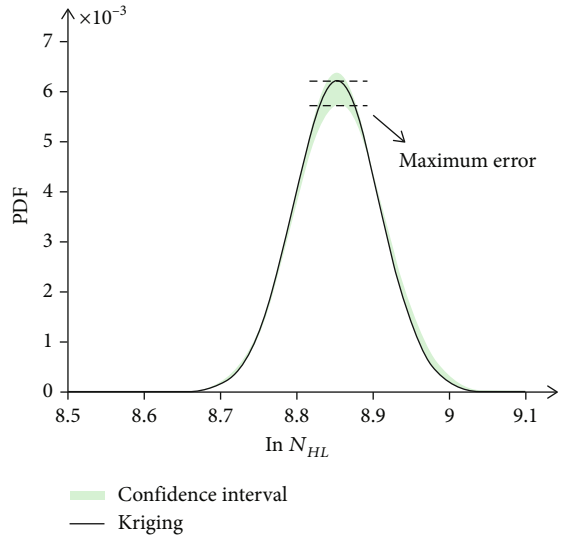

Figure 9: Comparison of MCS and Kriging (turbine blade).

Table 6: Turbine blade fatigue life prediction.

Reliability	Fatigue life (Kriging)	Fatigue life (MCS)	Relative error
0.5	6984.2(h)	7011.5(h)	0.38%
0.9	6508.8(h)	6486.7(h)	0.31%
0.99	6126.4(h)	6094.6(h)	0.52%

where N_{HL} is the H-LCF life; N_L and N_H are the LCF life and HCF life, respectively; A_{HL} and B_{HL} are the H-LCF fatigue coupling coefficient, $A_{HL} = 0.16$, $B_{HL} = 0.15$; a_{HL} is the H-LCF critical damage coefficient, $a_{HL} = 0.98$. Substituting N_L, N_H, and all parameters into the Eq. (5), the H-LCF life is $N_{HL} = 7013.03$h. It can be seen that the life of H-LCF is $|7013.03 - 7630/7630| = 8.1\%$ lower than that of LCF due to high cycle effect.

2.3. Fatigue Reliability Analysis. Generally, the influencing factors of fatigue life have objective uncertainty, which leads to the uncertainty of fatigue life. Therefore, it is necessary to analyze the fatigue reliability of turbine blade.

2.3.1. Uncertainty of Influencing Factors. For the fatigue reliability, there are six random input variables, including three rotational speeds of working states, Young's modulus, Poisson's ratio, and linear expansion coefficient. They are independent and normal distributed. The distribution parameters are listed in Table 5. The coefficient of variation (COV) of rotational speed is clearly required in the Aero-engine Life Determination Guide [28], which is less than 3% (COV of rotational speed is 0.02). The COV of material properties is determined [23] according to the aero-engine material manual.

2.3.2. Fatigue Reliability Analysis Methods. Fatigue reliability analysis studies the transfer law of uncertainty from influencing factors to the fatigue life. MCS is the classical reliability numerical simulation algorithm. MCS is based on the large number theorem. The process of MCS is that firstly the random samples of input variables are extracted M times according to the probability distribution and then substitute the input samples into the performance function to obtain M response values, and finally, the statistical analysis should be carried out by using M response values. However, there is no explicit performance function for the fatigue life of turbine blades, and the implicit relationship between influencing factors and the fatigue life can only be determined by finite element analysis. The finite element stress-strain analysis of the random input samples is carried out by ABAQUS and then substitute stress and strain into the H-LCF life prediction model to obtain the complex fatigue life. MCS is very time-consuming. In order to reduce the number of FEM, Kriging model is carried out to construct the surrogate model of influencing factors and fatigue life.

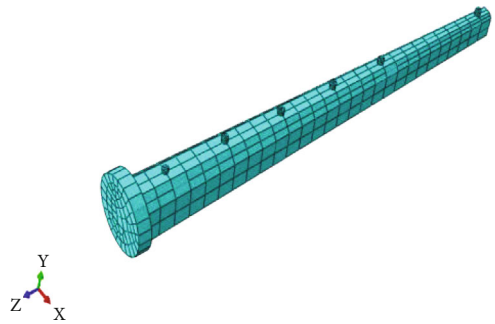

Figure 10: Finite element model of test probe.

Table 7: Probe frequency calculation results.

Mode	1st	2nd	3rd	4th	5th	6th
Frequency (Hz)	508.65	647.42	2025.5	2653.7	4852.5	5908.5

According to the training samples obtained from the distribution form of random variables, Kriging model can be established. And U learning function is adopted to update the Kriging model until it meets the accuracy requirement. Then, reliability analysis is performed based on the constructed Kriging model.

2.3.3. Fatigue Reliability Estimation Results. According to the distribution information of input influencing factors, MCS extracts 10000 H-LCF life samples by using finite element analysis 3×10000 times. Each FEM needs 50 s, so MCS to estimate the fatigue reliability needs at least $3 \times 50 \times 10000 = 1500000\,\text{s} \approx 17.4\text{days}$. The frequency distribution histogram of fatigue life can be obtained, as shown in Figure 8.

The logarithmic fatigue life $\ln N_{HL}$ of the turbine blade obeys the normal distribution. The 95% confidence interval of mean $\mu_{\ln N_{HL}}$ is (8.8502, 8.8585), and the 95% confidence interval of standard deviation $\sigma_{\ln N_{HL}}$ is (0.0598, 0.0614).

The Kriging surrogate model $N_{HL} = g_k(x)$ can be established for turbine blade. And the statistical parameters of the surrogate model are $\mu_{g_k} = 6984.2$ and $\sigma^2_{g_k} = 391.47^2$. Since N_{HL} is lognormal distribution, then

$$\text{Kriging} : \ln N_{HL} \sim N\left(8.8512, 0.0609^2\right). \tag{6}$$

To construct the Kriging model, it needs only 46 sample points, that is to say, $3 \times 50 \times 46\,\text{s} = 2300\,\text{s} \approx 1.92\text{h}$. The calculation time of FEM by MCS and Kriging is greatly shortened from "week" to "hour." The calculation time is greatly shortened. As shown in Figure 9, the sample distribution obtained by Kriging method is within the confidence interval of MCS estimation. There is the maximum error at the mean point, and the maximum error is 0.05%. The calculation accuracy also meets the requirements.

Given the design fatigue life N^*, the probability of turbine blade reliability can be evaluated, i.e., $\int_{N^*}^{+\infty} (1/x\sigma\sqrt{2\pi}) \exp\left[-1/2(\ln x - \mu/\sigma)^2\right]\mathrm{d}x$. The fatigue lives under different reliabilities are listed in Table 6. The errors of prediction results between Kriging model and MCS are all less than 1%, which proves the effectiveness of the surrogate model. And the fatigue reliability design can also be carried out based on the established Kriging model.

3. Fatigue Reliability Analysis of Test Probe

Test probe is an important test tool to test the parameters of vibration, air flow temperature, velocity, and pressure in the inner turbulent flow of aero-engine. In order to determine the replacement time of the probe, it is necessary to predict its fatigue life and estimate the fatigue reliability. The working load of the test probe is vibration excitation, which is low-stress and high-frequency. Therefore, the fatigue problem of the test probe belongs to high cycle fatigue. The fatigue reliability analysis of the probe includes finite element analysis to obtain the RMS stress of dangerous position, HCF life prediction model, and fatigue reliability analysis.

3.1. Finite Element Analysis. The finite element analysis process of the test probe [22] is similar to that of turbine blade (shown in Figure 1), but it is different from turbine blade in terms of working environments, stress characteristics, and fatigue damage modes.

3.1.1. Parametric Modeling. The inside of the test probe is hollow. Sensors, internal hoses, etc. can be installed inside the probe. The bottom of test probe is usually fixed on the inlet cylinder wall by bolts. Simplifying the chamfers, external pressure pipe nozzles, and other relevant parts, the model of probe is simplified to a typical cantilever beam structure [29]. The finite element model of probe (shown in Figure 10) is meshed by ABAQUS.

The material of the test probe is 1Cr18Ni9Ti steel, and the material parameters [30] are listed as follows: the density is 7850kg/m^3, the elastic modulus is 184000 MPa, and the Poisson's ratio is 0.31.

3.1.2. Mechanics Analysis

(1) Load Analysis. The test probe mainly bears the aerodynamic pressure load and vibration load.

(1) Aerodynamic pressure load

When the air flow enters the inlet of aero-engine, the pressure different is generated on the windward and leeward of test probe. Therefore, the aerodynamic load is applied to the probe. The aerodynamic load can be simplified into distributed pressure, which can be applied through the static analysis module of ABAQUS.

(2) Vibration load

Vibration load includes the load transmitted by inlet cylinder wall vibration and aerodynamic excitation force. The vibration load of the probe is complex and belongs to random load. Using the long-time flight test data, we can obtain the working time and average frequency of the probe and

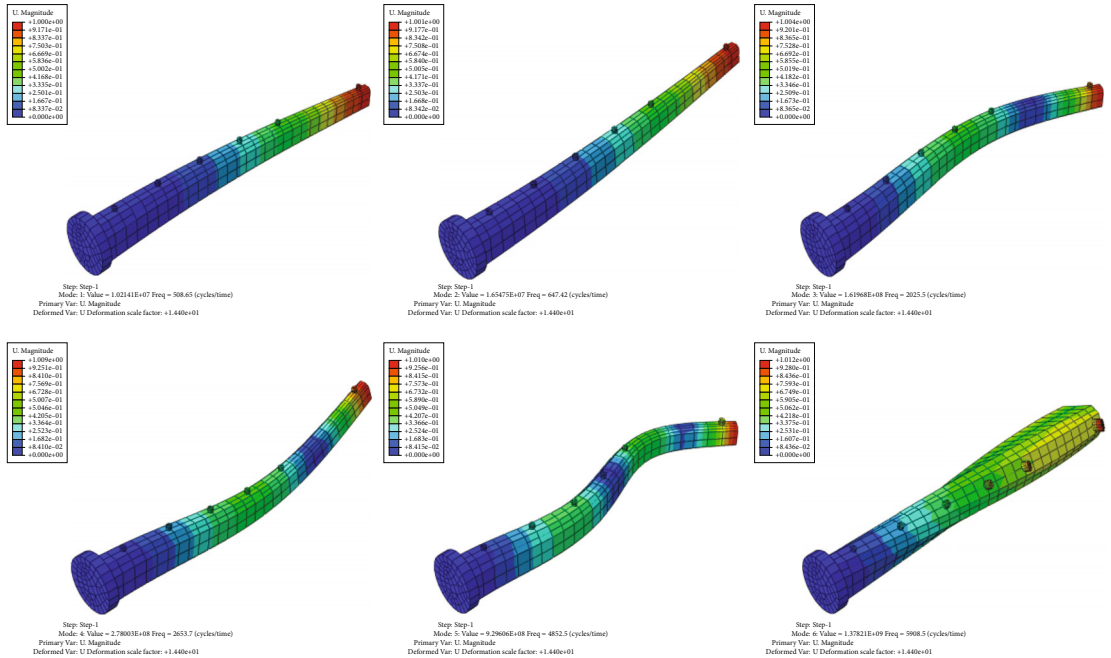

Figure 11: The 1st to 6th order mode shape diagrams of test probe.

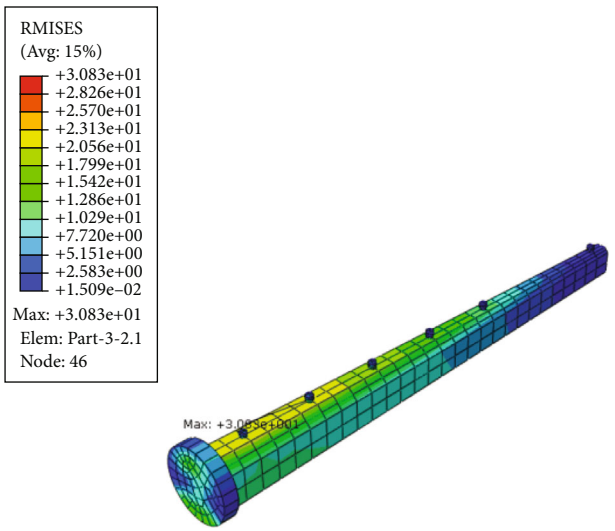

Figure 12: RMS stress cloud diagram of test probe.

Table 8: Fatigue life under three stress levels.

$N_{1\sigma}$	$N_{2\sigma}$	$N_{3\sigma}$
8.3486×10^{19}	1.5310×10^{13}	1.9384×10^{9}

then obtain the PSD of excitation force, which is applied in the random response analysis module of ABAQUS.

3.1.3. Dynamic Finite Element Analysis

(1) Modal Analysis. When the frequency of external load is close to the natural frequency of test probe, resonance will occur. The modal analysis of test probe is carried out to obtain the natural frequencies (listed in Table 7) and mode shapes (seen in Figure 11).

(2) Random Response Analysis. The variation of vibration load caused by probe base vibration and aerodynamic excitation force is relatively complex [31], which is analyzed by frequency domain method based on PSD. For random response analysis, the frequency range is generally set to $0 \sim 2000$ Hz, and the probe modal damping is set to 0.05. The RMS stress distribution of random vibration response of the probe can be solved by ABAQUS, as shown in Figure 12.

3.2. High Cycle Fatigue Life Prediction. Steinberg's three-interval method [27] is used to solve the HCF life of test probe. The equivalent RMS stress of test probe in Figure 12 and the fitted S-N curve [23] of 1Cr18Ni9Ti steel are as follows.

$$S^m N = C, \tag{7}$$

where m and C are the fitting parameters, $m = 22.34$ and $C = 1.6^{50}$. The cycle number $N_{1\sigma}$, $N_{2\sigma}$, and $N_{3\sigma}$ can be obtained, respectively, and listed in Table 8.

Take the vibration time $T = 700$ hour and the vibration frequency $f = 508.65$ Hz, substitute all data into the life prediction Eq. (4), and the HCF life of the probe is $N_H = 10042.3$ hours.

3.3. Fatigue Reliability Analysis. The fatigue life of the test probe is affected by random influencing factors, resulting in great variability of fatigue life. In order to better predict the fatigue life, it is necessary to analyze the fatigue life reliability of the test probe.

Table 9: Statistical characteristics of random variables.

Random variables	Distribution type	Mean value	Coefficient of variation
Aerodynamic pressure P (MPa)	Normal	3.5	0.02
Young's modulus E (MPa)	Normal	184000	0.01
Poisson's ratio	Normal	0.31	0.01

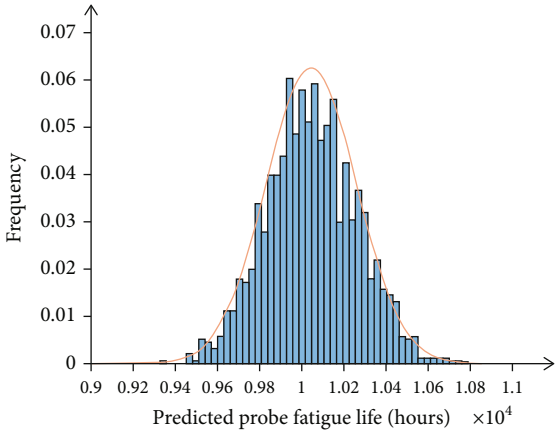

Figure 13: Distribution of probe fatigue life sample (Monte Carlo method).

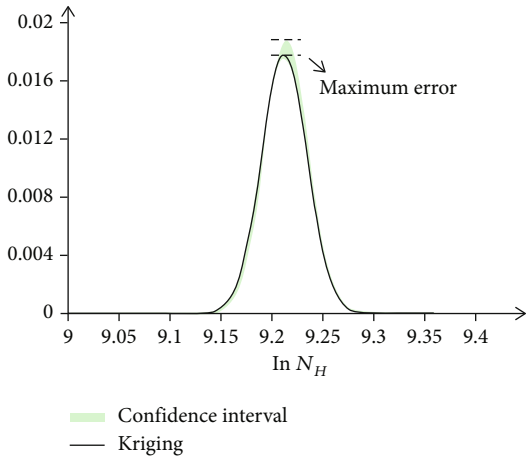

Figure 14: Comparison of MCS and Kriging (test probe).

Table 10: Test probe fatigue life prediction.

Reliability	Fatigue life (Kriging)	Fatigue life (MCS)	Relative error
0.5	10049.8(h)	10023.4(h)	0.26%
0.9	9719.1(h)	9775.6(h)	0.58%
0.99	9482.2(h)	9554.5(h)	0.76%

3.3.1. Uncertainty of Influencing Factors. The aerodynamic pressure and material properties of the test probe are selected as the input random variables. The mean value and variation coefficient of the random variables come from the statistical analysis of the test data [31]. The distribution types and distribution parameters of the random factors are shown in Table 9.

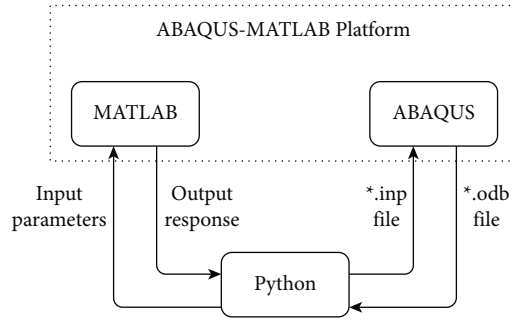

Figure 15: System structure diagram.

3.3.2. Fatigue Reliability Estimation. 10000 groups of HCF predicted life samples of probe are obtained, and then MCS is used for probabilistic statistical analysis. The frequency distribution histogram can be obtained, as shown in Figure 13. And because each FEM takes 31 seconds to get the stress, MCS needs about 31s × 10000 = 310000 s ≈ 3.5days.

The logarithmic fatigue life $\ln N_H$ of the test probe obeys the normal distribution. The 95% confidence interval of mean $\mu_{\ln N_H}$ is (9.2118, 9.2138), and the 95% confidence interval of standard deviation $\sigma_{\ln N_H}$ is (0.0216, 0.0239).

A Kriging surrogate model $N_H = g_k(x)$ is established for test probe. And the statistical parameters of the surrogate model are $\mu_{g_k} = 10049.8$ and $\sigma^2_{g_k} = 224.66^2$. Since N_H is log-normal distribution, then

$$\text{Kriging} : \ln N_H \sim N\left(9.2125, 0.0224^2\right). \tag{8}$$

In order to establish the Kriging model, 35 sample points need to be used. It only takes about 20 minutes. As shown in Figure 14, the sample distribution obtained by Kriging method is within the confidence interval of MCS estimation. There is the maximum error at the mean point, and the maximum error is 0.02%. The test probe fatigue lives under different reliabilities are shown in Table 10. The error of estimations between Kriging model and MCS is less than 1%.

4. Fatigue Reliability Analysis System

ABAQUS finite element software is widely used because of its powerful modeling and intuitive cloud diagram display, simple Python kernel language, and strong interfaces. MATLAB is a powerful tool language for engineering mathematics analysis and calculation. It is favored because of

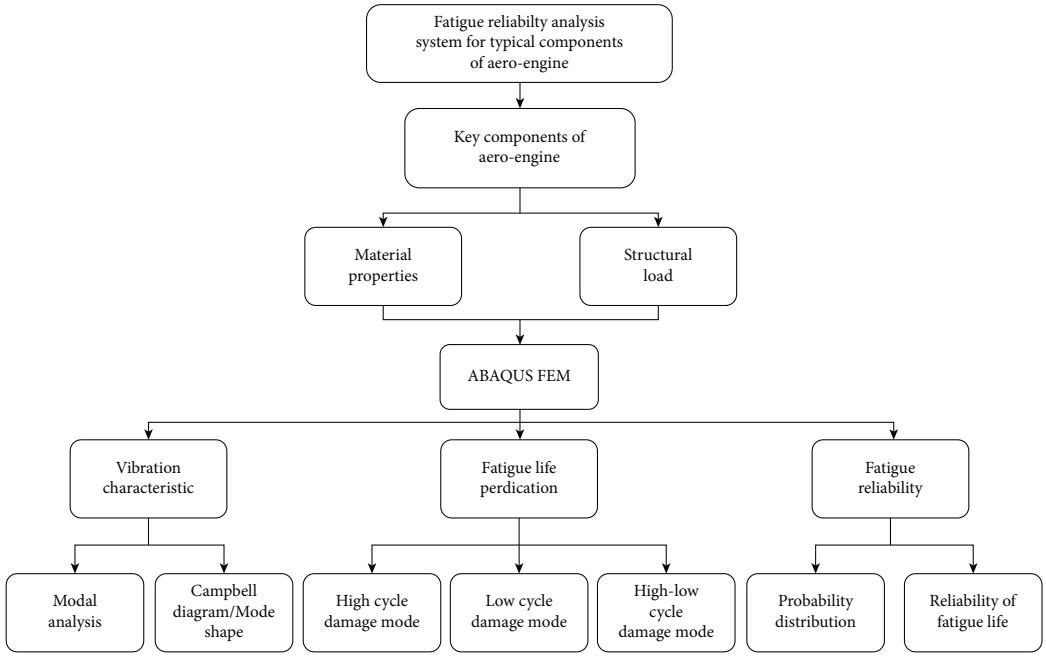

Figure 16: System operation flowchart.

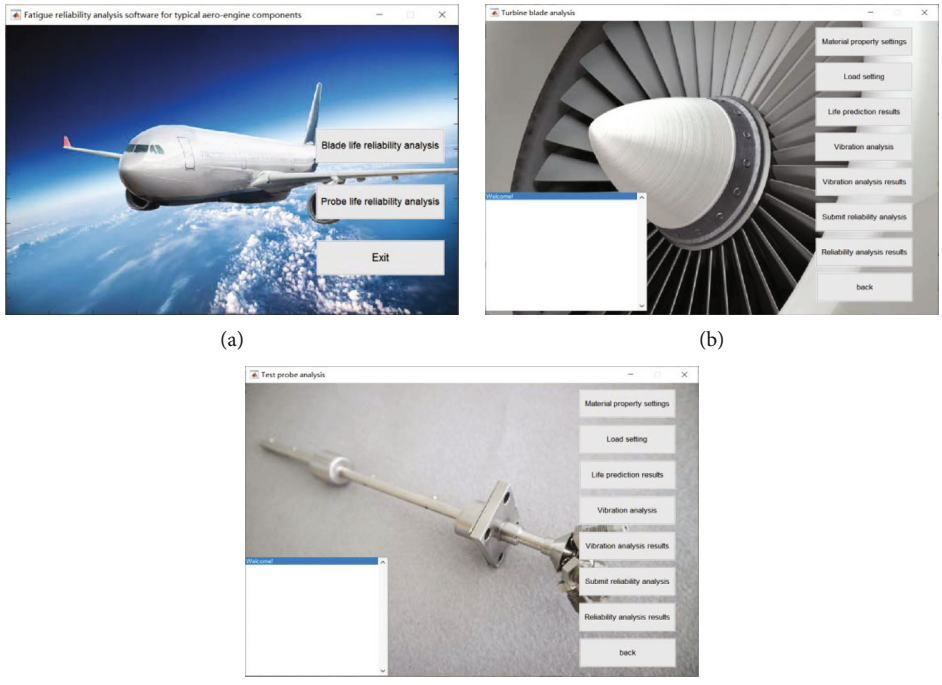

Figure 17: System interfaces.

its good at processing matrices and vectors. The fatigue reliability analysis of turbine blade and test probe indicates that fatigue reliability analysis is a complicated but relatively fixed process. Therefore, we develop a fatigue life reliability analysis system based on ABAQUS-MATLAB platform for aero-engine turbine blade and test probe. The developed system can be operated conveniently and quickly, and its results are believable and accuracy.

4.1. Structure of Fatigue Reliability System. The ABAQUS-MATLAB platform needs Python as a bridge. The information between ABAQUS and MATLAB include the input parameters (such as E and ρ) and output response (such as σ and ε). And Python is used to make preprocessing and postprocessing of ABAQUS, i.e., import the *.inp file and export the *.odb result file. The structure of ABAQUS-MATLAB platform is shown in Figure 15.

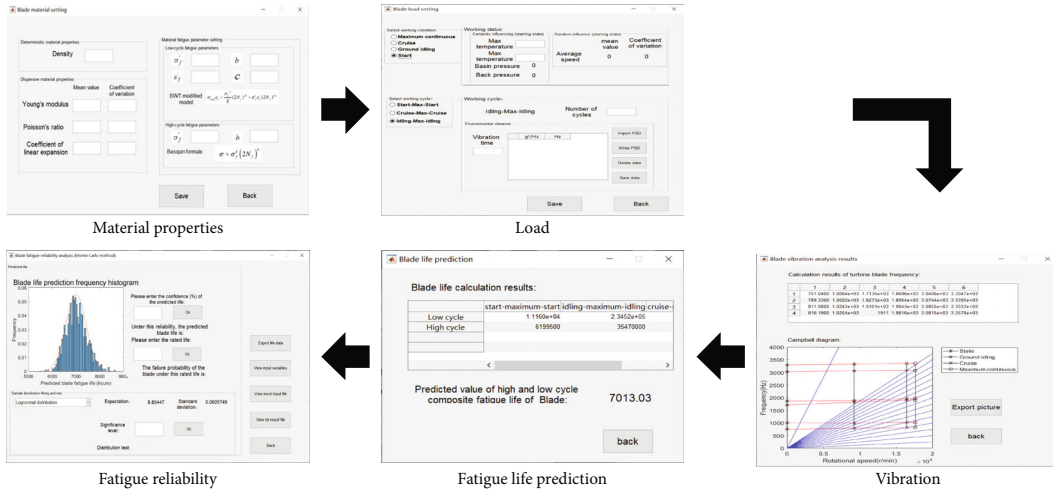

Figure 18: The analysis process for turbine blade.

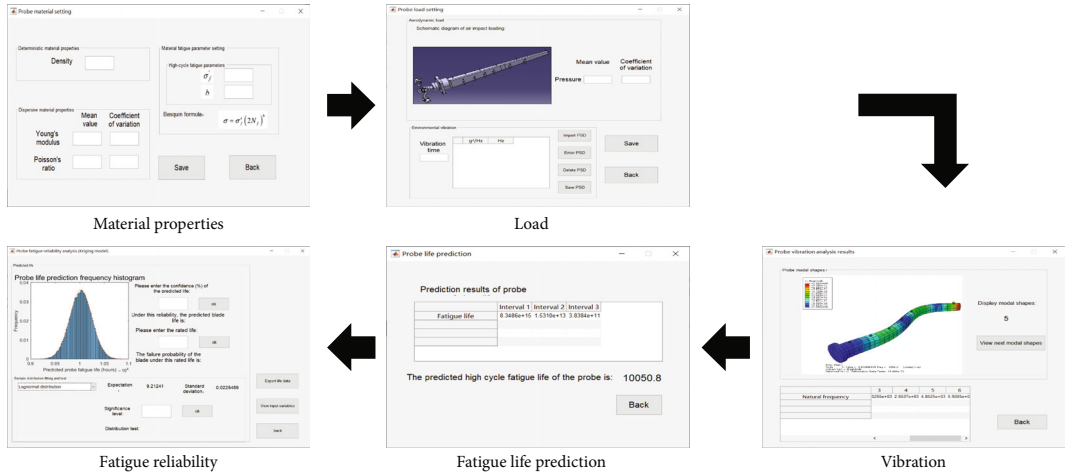

Figure 19: The analysis process for test probe.

ABAQUS-MATLAB platform is associated with the following four technical points:

(1) Generate the basic *.inp file of ABAQUS

The operation commands of ABAQUS for preprocessing modeling will be recorded in abaqus.rpy file, which is a script in Python language format. And the input file can be edited and submitted to ABAQUS by Python.

(2) Automatically rewrite input file by MATLAB

Set keywords and the positions in advance. MATLAB imports the input parameter sample and calls the Python code to rewrite the abaqus.rpy. Name the rewritten script file abaqus.py, which is convenient for automatic repeat calls.

(3) Call ABAQUS for FEM by MATLAB

Use the system() function in MATLAB, and run the following code:

```
system('abaqus cae noGUI=abaqus.py')
```

Note that ABAQUS should be called asynchronously.

(4) Read the result file and import to MATLAB

Take the output of the maximum principal strain in ABAQUS result *.odb file as an example, run the following Python code:

```
session.writeFieldReport(.
fileName = 'temp.txt',
outputPosition = INTEGRATION_POINT,
variable = (('LE',INTEGRATION_POINT, ((INVARIANT, 'Max. Principal'),)),))
```

"Variable" is the type of the extracted variable, and "output Position" is the output position of the variable. Then import the maximum principal strain value to MATLAB and save it for statistical analysis.

4.2. Operation Flow of Fatigue Reliability Analysis System. The system includes the parametric finite element modeling,

finite element analysis of vibration characteristics, life prediction, and fatigue life reliability analysis for the aero-engine turbine blade and test probe. The system running flowchart is shown in Figure 16.

The main interface of the system is shown in Figure 17(a). Click the button to open the interfaces of blade and probe (in Figures 17(b) and 17(c), respectively).

There are analysis processes arranged in the interface Figures 17(b) and 17(c). Click the buttons in turn, import or input the required information in the corresponding interface, and finally obtain the prediction fatigue life and fatigue reliability results of blade and probe, shown in Figures 18 and 19.

It can be seen that the developed system has simple operation and strong practicability. The system can also be used for the analysis of aero-engine casing, turbine shaft, and other key components.

5. Conclusions

Turbine blade and test probe are key components of aero-engine, and their fatigue life and reliability are related to the economy and safety of the aircraft. Based on the ABAQUS finite element analysis model, using the Miner's linear fatigue damage accumulation theory, combined with the S-N curve of materials and performance parameters, the fatigue reliability analysis of aero-engine's key components has been realized and programmed. The fatigue reliability analysis system is developed based on the ABAQUS-MATLAB platform. The system includes four modules: parametric finite element modeling, finite element vibration characteristics analysis, fatigue life prediction, and fatigue life reliability analysis. Under different reliability requirements, the fatigue life prediction results between Kriging model and MCS are consistent, which meets the analysis accuracy requirement. And Kriging can significantly reduce the calculation time. This system provides a more convenient way for the fatigue life reliability analysis of key aero-engine components, which can meet actual engineering requirements and accelerate the design speed of aero-engine's key components. In addition, the designed system reserves interfaces for embedding other component analysis modules and reliability analysis methods.

Data Availability

The simulation data used to support the results of this study are included in this paper.

Conflicts of Interest

The authors declare that they have no conflicts of interest.

References

[1] L. Han, P. Li, S. Yu, C. Chen, C. Fei, and C. Lu, "Creep/fatigue accelerated failure of Ni-based superalloy turbine blade: microscopic characteristics and void migration mechanism," *International Journal of Fatigue*, vol. 154, article 106588, 2022.

[2] Z. An, "Development of structural strength test technology for aviation turbofan engine," *Aeroengine*, vol. 47, no. 4, pp. 131–140, 2021.

[3] W. Yao, *Structural Fatigue Life Analysis*, Science Press, Beijing, 1st edition, 2019.

[4] X. Pei, X. Li, S. Zhao, P. Dong, X. Liu, and M. Xie, "Low cycle fatigue evaluation of welded structures with arbitrary stress-strain curve considering stress triaxiality effect," *International Journal of Fatigue*, vol. 162, article 106969, 2022.

[5] P. Yue, J. Ma, C. Zhou, J. Hao, and P. Wriggers, "A fatigue damage accumulation model for reliability analysis of engine components under combined cycle loadings," *Fatigue & Fracture of Engineering Materials & Structures*, vol. 43, no. 8, pp. 1880–1892, 2020.

[6] L. Han, Y. Wang, Y. Zhang, C. Lu, C. Fei, and Y. Zhao, "Competitive cracking behavior and microscopic mechanism of Ni-based superalloy blade respecting accelerated CCF failure," *International Journal of Fatigue*, vol. 150, article 106306, 2021.

[7] X. Zhang, Y. Liu, and O. Caglar, "Multiscale reduced-order modeling of a titanium skin panel subjected to thermomechanical loading," *AIAA Journal*, vol. 60, no. 1, pp. 302–315, 2021.

[8] T. You, J. Zhou, D. Gong, Y. Sun, B. Li, and J. Chen, "Synthesis of random vibration environment spectra for the fatigue analysis and optimization of railway vehicles," *International Journal of Fatigue*, vol. 159, article 106752, 2022.

[9] N. Somanath, R. Noraas, M. Giering, and O. Oshin, "Structural material property tailoring of dual phase titanium alloy microstructures using deep neural networks," in *AIAA 2020-1151. AIAA Scitech 2020 Forum*, Orlando, FL, January 2020.

[10] S. Yu and J. Ou, "Fatigue life prediction for orthotropic steel deck details with a nonlinear accumulative damage model under pavement temperature and traffic loading," *Engineering Failure Analysis*, vol. 126, article 105366, 2021.

[11] S. Zhu, S. Foletti, and S. Beretta, "Probabilistic framework for multiaxial LCF assessment under material variability," *International Journal of Fatigue*, vol. 103, pp. 371–385, 2017.

[12] D. Hu, X. Su, X. Liu, J. Mao, X. Shan, and R. Wang, "Bayesian-based probabilistic fatigue crack growth evaluation combined with machine-learning-assisted GPR," *Engineering Fracture Mechanics*, vol. 229, article 106933, 2020.

[13] X. Niu, R. Wang, D. Liao, S. Zhu, X. Zhang, and B. Keshtegar, "Probabilistic modeling of uncertainties in fatigue reliability analysis of turbine bladed disks," *International Journal of Fatigue*, vol. 142, article 105912, 2021.

[14] X. Li, L. Song, and G. Bai, "Recent advances in reliability analysis of aeroengine rotor system: a review," *International Journal of Structural*, vol. 13, no. 1, pp. 1–29, 2022.

[15] X. Liu, J. Liu, H. Wang, and X. Yang, "Prediction and evaluation of fatigue life considering material parameters distribution characteristic," *International Journal of Structural*, vol. 13, no. 2, pp. 309–326, 2022.

[16] C. Fei, H. Li, H. Liu et al., "Enhanced network learning model with intelligent operator for the motion reliability evaluation of flexible mechanism," *Aerospace Science and Technology*, vol. 107, article 106342, 2020.

[17] Z. Lu, S. Song, L. Li, and Y. Wang, *Structure/Mechanism Reliability Design Basis*, Northwestern Polytechnical University press, Xi'an, 1st ed edition, 2019.

[18] D. Wang, C. Hua, D. Dong, B. He, and Z. Lu, "Crack parameters identification based on a kriging surrogate model for

operating rotors," *Shock and Vibration*, vol. 2018, Article ID 9274526, 12 pages, 2018.

[19] C. Tong, J. Wang, and J. Liu, "A kriging-based active learning algorithm for mechanical reliability analysis with time-consuming and nonlinear response," *Mathematical Problems in Engineering*, vol. 2019, Article ID 7672623, 14 pages, 2019.

[20] Y. Wang, Z. Han, Z. Yang, C. Lu, and X. Xue, "Time-varying reliability analysis of compressor blisk based on particle swash optimization extreme kriging model," *Journal of Northwestern Polytechnical University*, vol. 39, no. 6, pp. 1240–1248, 2021.

[21] C. Lu, C. Fei, Y. Feng, Y. Zhao, X. Dong, and Y. Choy, "Probabilistic analyses of structural dynamic response with modified kriging- based moving extremum framework," *Engineering Failure Analysis*, vol. 125, article 105398, 2021.

[22] W. Qi, *ABAQUS 6.14 Super Learning Manual*, Post & Telecom press, Beijing, 1st ed edition, 2016.

[23] Editorial Committee of China Aviation Materials Manual, *Handbook of Aeronautical Materials of China (Volume II) Wrought and Cast Superalloys*, China Standard Press, Beijing, 1st ed. edition, 2001.

[24] W. Peng, X. Huang, X. Zhang, L. Ni, and S. Zhu, "A time-dependent reliability estimation method based on surrogate modeling and data clustering," *Advances in Mechanical Engineering*, vol. 11, no. 4, Article ID 1687814019839874, 8 pages, 2019.

[25] D. Ali, A. Shahzad, and T. A. Khan, "Development of fatigue loading spectra from flight test data," *Procedia Structural Integrity*, vol. 2, pp. 3296–3304, 2016.

[26] L. Yan, Z. Zhu, Z. Song, Q. Li, and F. Liu, *Analysis of Dynamic Characteristics of Structural System*, Beihang University Press, Beijing, 1st ed. edition, 1989.

[27] X. Wang, Z. Wang, J. Wang, Y. Hu, and S. Han, "Random vibration fatigue analysis of UAV engine support based on Steinberg method," *Electrical and Automation*, vol. 50, no. 6, pp. 216–219, 2021.

[28] Q. Su, *Life Determination Guide for Main Components of Aero Turbojet and Turbofan Engines*, Aviation Industry Press, Beijing, 1st ed. edition, 2004.

[29] J. Liu, *Researches on the Numerical Simulation and Fatigue Life Prediction Methods of Response Characteristicsof Thin-Walled Structures via FEM, Ph. D. Dissertation*, Dept. of mechanical electronics, Electronic Science and Technology Univ, Chengdu, 2011.

[30] Editorial Committee of China Aviation Materials Manual, *Handbook of Aeronautical Materials of China (Volume I) Wrought and Cast Superalloys*, China Standard Press, Beijing, 1st ed. edition, 2001.

[31] Z. Zuo, R. Wu, and B. Guo, "The fatigue life of aero-engine total pressure probe on the base excitation," *Journal of Mechanical Strength*, vol. 37, no. 2, pp. 355–359, 2015.